An Outlook into a Possible Intensified Camera Based Thomson Scattering System for High Temperature Plasmas*)

Kiyong LEE

Plasma Technology Research Center, National Fusion Research Institute, Gunsan 573-540, Korea

(Received 11 September 2018 / Accepted 9 December 2018)

A possible intensified camera based Thomson scattering (TS) system for high temperature plasma measurement of over 100 eV is investigated. The TS system is not specific to a certain device, but can be applicable to any plasma source capable of producing high temperatures with densities of over $1 \times 10^{19}/\mathrm{m}^{-3}$ range. A code has been developed to estimate the number of collectable scattered photons and its corresponding photoelectrons. The system uses an sCMOS intensified camera, which comes with many convenient features in terms of precise timing, digitization, and its compactness. Due to the broad wavelength range of the scattering spectrum, to increase detection of photons per pixel, the optical setup have to compromise of the most efficient element that uses volume phase holographic (VPH) grating and a wire grid polarizer. Off-the-shelf components have been chosen for the VPH spectrometer, intensified camera, and the 532 nm Nd:YAG laser that is available up to 5 J/pulse without custom request. Two separate magnification ratio 1:2 and 1:3 of the collection lens are considered for estimating the TS signal during a single laser shot.

Keywords: Thomson scattering, plasma, Nd:YAG laser, high temperature, intensified camera

DOI: 10.1585/pfr.14.2401019

1. Introduction

From experience gained on developing a Thomson scattering (TS) system that uses a triple-grating spectrometer with an ICCD camera for low temperature (below 10 eV) plasma measurements [1], a code was written to estimate the detected signal levels. It is shown to match well with experimental measurements, and gives confidence on the value of multiple elements (optical transmission, detector quantum efficiency, noise, etc.) that provide useful information for constructing a similar TS system.

We focus attention towards high temperature plasmas of over 100 eV by using recent off-the-shelf components that enables the TS system to collect interpretable data in a single laser shot by using moderate laser energy of 1.5 J/pulse as compared with former studies [2, 3] of over 15 J/pulse. The system uses a volume phase holographic (VPH) transmission grating that has a similar setup as with the TS system for the Pegasus Toroidal Experiment [4]. However, to collect more scattering photons, single core optical fibers are in use to eliminate package spacing and advantages of pixel binning from the sCMOS sensor are taken into consideration. In addition, convolution effects are included to predict the estimated photoelectrons for the proposed TS system.

For low temperature plasmas, the scattering spectrum is of a few nm width. The optical properties are estimated to have a single constant value. However, for high temperatures the spectrum is much wider and must account for differences as a function of wavelength. Whereas low temperature TS systems require fine optical resolution with the cost of losing optical throughput (or etendue), high temperature TS is quite the opposite. That is maximize throughput while allowing less resolution.

Having identical scattering geometry, two separate designs that differ in the magnification ratio of the collection lens are considered. At first, using 1064 nm Nd:YAG laser in the near infrared (NIR) region have been considered. However, the quantum efficiency (QE) at NIR with the Gen III image intensifier is at most 4%, which does not offer practical usage. Thus, we concentrate on the visual (VIS) region of the spectrum by scattering of 532 nm wavelength.

2. Optical Components and Nd: YAG Laser

An efficient optical system requires less optical components while increasing the optical throughput. The design is specific to the HoloSpec-F/1.8-VIS (Andor) spectrometer that uses a VPH transmission grating.

The entrance numerical aperture (NA) of 0.28 allows acceptance of the light cone angle to be more than typical spectrometers. Due to the high NA, the shortened focal length causes image distortion at the sensor location. Thus special lenses are in place at the input and output side of the VPH spectrometer for image correction providing multi-track capabilities. The nominal dispersion is 16.15 nm/mm

---

author's e-mail: kylee@nfri.re.kr

*) This article is based on the presentation at the 12th International Conference on Open Magnetic Systems for Plasma Confinement (OS2018).

(VPH grating model: HS-HVG-590), where measureable wavelength range from 367 to 813 nm. Including the grating and lenses, the transmission of the spectrometer is expected to be ~60%.

The closest match to the NA of the VPH spectrometer is by using optical fibers of pure fused silica core with fluorine doped silica cladding that has NA of 0.26. The optical throughput of the TS system is determined by the solid angle Ω (from fiber NA) multiplied by the fiber core area S.

In Fig. 1, the geometry setup for the collection lens is shown. The collection lens front is placed 500 mm away from the scattering point. For design purpose a single point at 90° scattering is investigated. The clear aperture of the collection lens is determined by matching the throughput of the optical fiber $S_{\text{fiber}}\Omega_{\text{fiber}} = S_{\text{object}}\Omega_{\text{object}}$. Two collection lens that differs by the magnification ratio of 1:2 or 1:3 are considered. Each corresponds to a single fiber core diameter of ϕ1500 μm and ϕ1000 μm to image the scattered light from the ϕ3 mm laser beam diameter. We assume that the collection lens consists of 5 elements, each with 95% transmission. At the end of the collection lens, a wire grid polarizer (450 ~ 700 nm) having 87% transmission is attached. When including the port window (90%) leads to the combined transmission of 60% before photons enter into the optical fiber.

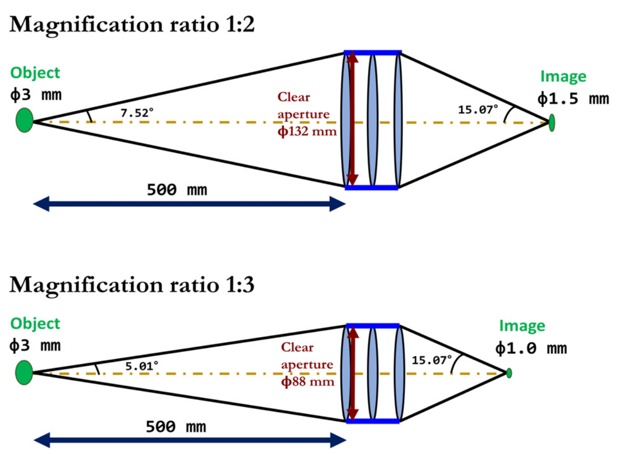

Fig. 1 Geometry for the collection lens, which differs by the magnification ratio of 1:2 and 1:3.

Although it may be possible to increase the performance of the laser upon request, commercially available Nd:YAG lasers at 532 nm are considered. Lasers at frequency of 10 Hz with energy from 1.5 up to 5.0 J are available. We specifically concentrate on the 1.5 J laser to focus at the lower limit, since scattered light is directly proportional to the laser energy. A summary of the optical components are listed in Table 1.

3. Intensified Camera

Fast gating of a few ~ ns and signal amplification are two essential features needed to capture scattered photons. The image intensifier unit attached in front of the camera allow these two essential features. Making the transfer from photon to photoelectron by the photocathode, the QE of the detector is depicted by the image intensifier, where one can expect 50% QE at 500 nm by using Gen III.

To record the amplified signal, a variety of sensors are available, in which enhancements are likely to improve due to its wide usage. At first, the CCD sensor would be the likely choice. However, recent advancements in semiconductor technology have brought a diverse range of sensors into the market that provide advanced capabilities over the CCD.

Table 2 shows major characteristics of several different sensors. The CCD array holds a wide range of products that varies by the array size and wavelength sensitivity. The sCMOS sensor is the probably the most favorable choice due to the fast frame rate at low readout noise with

Table 1 Specifications and transmission of optical components used for the TS system.

	Specifications		Transmission (%)
Laser	Nd:YAG@532 nm, 1.5 J/pulse		
Spectrometer	Volume Phase Holographic transmission grating		~ 60
Collection lens (f = 500 mm) magnification ratio	1:2	1:3	77 (consisting of five lenses)
Clear aperture diameter	ϕ 132 mm	ϕ 88 mm	
Solid angle	0.054 sr	0.024 sr	
Optical fiber core diameter	1500 μm	1000 μm	99.7
Wire grid polarizer	450 ~ 700 nm		87
Port window	Borosilicate Glass		90

Table 2 Characteristics of several sensors used on the intensified camera. (Data from Hamamatsu and Andor catalog).

	CCD	sCMOS	EM-CCD	InGaAs
Quantum Efficiency	70%@500 nm 300~1100 nm	82%@560 nm 400~1100 nm	90%@550 nm 300~1100nm	60%@1250 nm 900~1700 nm
Effective number of pixels and size	1344(H)×1024 (V) 8.67 × 6.60 mm² 6.45 μm square	2048(H)×2048 (V) 13.3 ×13.3 mm² 6.5 μm square	1024(H)×1024 (V) 13.3 ×13.3 mm² 13 μm square	640(H)×511 (V) 12.8 ×10.24 mm² 20 μm square
Frame rate (1 ×1 binning)	12.2 frames/s	40 frames/s	18.5 frames/s	7.2 frames/s
Readout noise (r.m.s)	10 electrons	1.4 electrons	1 (with EM gain) electrons	500 electrons
Exposure time	4.5 ms to 1 s	10 μs to 10 s	10 μs to 10 s	16.7 ms to 1 s
Features	Wide variety of products	Fast frame rate High image resolution	Amplification gain (1200×)	NIR range

high image resolution. The recent EM-CCD capable of single photon detection offer signal amplification but lacks fast gating, in which an image intensifier must be used. The InGaAs sensor possess a rather remarkable QE of 60% that remains nearly constant in the NIR wavelength region from 900 ~ 1700 nm. However, there is presently no image intensifier that covers this range, thus leaving the usage of 1064 nm Nd:YAG laser to the near future.

Although there exists similar devices, the design is specific on the iStar sCMOS camera (Andor). The sensor consists of 2560 (H) × 2160 (V) pixels, which is 16.6 mm × 14.0 mm in size. Having the optical fibers arranged in a straight linear array, the VPH spectrometer with 1:1.13 magnification images the fiber array towards the camera. With core size ϕ1500 µm it is possible to fit 7 fibers for multi-point measurements at 7 locations. By using ϕ1000 µm allow 11 fibers to be fitted. Having several parallel spectrometers could even enable more points to be measured. By nominal dispersion of 16.15 nm/mm, depicted by the horizontal sensor size, 444 ~ 708 nm is the measurable wavelength range that has been chosen to match with the specification of the wire grid polarizer.

4. Estimation of Scattered Signal

The signal is expressed in terms of photoelectrons, since the amplification factor can differ from various intensified camera models. The number of collected photoelectrons (ΔN_{pe}) in a wavelength interval $\Delta\lambda$ is by the following

$$N_{\mathrm{pe}}(\lambda) = \frac{E_{\mathrm{i}}}{h\upsilon_{\mathrm{i}}} \cdot n_{\mathrm{e}} \cdot \Delta L \cdot \frac{\Omega}{4\pi} \cdot \sigma_{\mathrm{TS}} \cdot S(\lambda) \cdot T(\lambda) \cdot QE(\lambda) \cdot \Delta\lambda, \quad (1)$$

where, E_{i} is the laser energy (J), h is Planck's constant, υ_{i} is the laser frequency, n_{e} is the electron density, $\varDelta L$ is the length of the measured plasma, $\varOmega$ is the solid angle, σ_{TS} is the Thomson scattering cross-section, $T(\lambda)$ is the transmission of the TS system, and $QE(\lambda)$ is the quantum efficiency by the image intensifier photocathode. For $S(\lambda)$, the relativistic scattering form factor, Selden's formula is used [5]. In its original form, $\int S(\lambda)d\lambda$ does not normalize to one. Thus, we divide it by a normalizing factor of $532 + 0.004275 \cdot T_{\mathrm{e}}$ (eV)-0.198736, which shows slight dependency on T_{e} and is only applicable to scattering of 532 nm wavelength. Integrating Eq. (1) for all wavelengths lead to the total number of collected N_{pe}. The result is shown in Fig. 2 for two magnification ratio of 1:2 and 1:3.

Binning of 32 horizontal pixels have been applied based on the 1 × 1 binning to indicate a single wavelength. The expected scattering signal is set for $n_{\mathrm{e}} = 1.0 \times 10^{19}\,\mathrm{m}^{-3}$ from T_{e} of 100 eV to 3 keV with a single laser shot. The center green vertical line indicates the laser wavelength. Adjacent are two lines, left and right, showing the estimated spectrometer resolution. For the VPH spectrometer with 50 µm slit, the resolution (FWHM) is 0.96 nm. With the fiber core diameter being the entrance slit-width, the resolution is estimated to increase linearly.

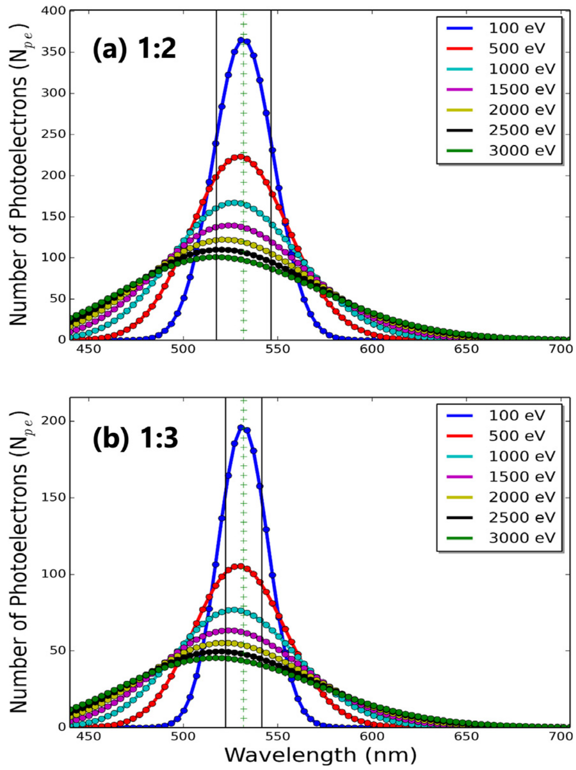

Fig. 2 Estimated number of photoelectrons for magnification ratio of (a) 1:2, and (b) 1:3. Convolution effects have been included.

Due to the large bandwidth of the resolution, after collecting the experimental data, convolution effects need to be addressed in order to assess the final T_{e} measurement. Instead of performing a direct deconvolution, matching with a tabled data set that includes convolution of the instrumental broadening is suggested.

To determine the signal-to-noise ratio (SNR), photon statistics is used. The excessive noise factor of the intensified camera that arises from randomly generated electrons being amplified by the image intensifier rarely occurs. Thus its effect can be ignored. The estimated SNR is shown in Fig. 3.

A horizontal line shown on the figure is to indicate SNR of 2. Any plotted curve that falls below this line is most likely unable to be distinguish as signal. When both Fig. 2 and Fig. 3 are compared, the signal difference in terms of the total number of photoelectrons is twice larger for (a) 1:2 than (b) 1:3. On the other hand, SNR going as the square root number of photons shows about 30% difference. This indicates that the improvement is less when the quality of the SNR is taken into account.

For temperatures over 2 keV, distinguishing the scattering curve becomes obscure. In this case, by binning more pixels could allow interpretation of the data to be similar to that of the polychromator.

One important factor that has not been considered is background subtraction, which would be appropriate to

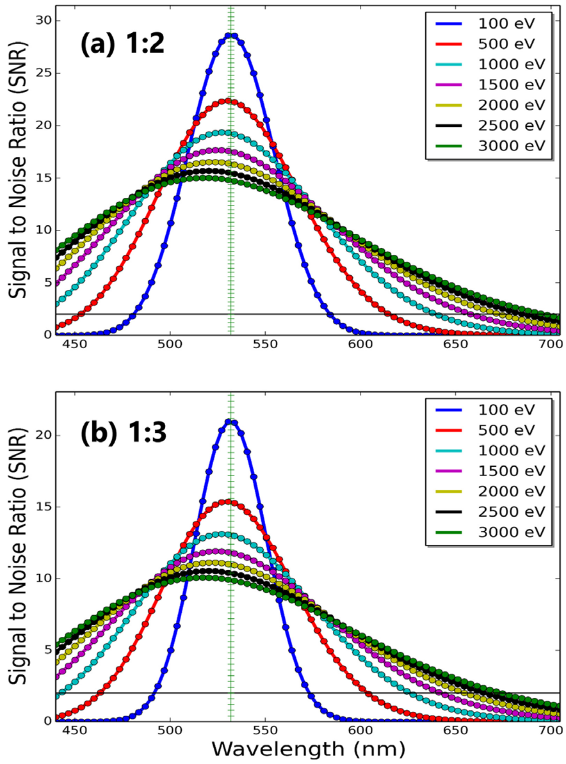

Fig. 3 Signal to noise ratio for magnification ratio of (a) 1:2, and (b) 1:3.

base it on direct experimental data. In general, high temperature plasmas are considered to be noisy due to the combination of line radiation, bremsstrahlung, and blackbody radiation from the vacuum wall being heated by the hot plasma.

There are two ways to subtract the background signal. The first is by having a fiber positioned next to the fiber that is used for measurement [4]. The observed geometry is not quite exact, but considered close enough. The advantage is that both scattering and background data are simultaneously collected at the same time. However, the number of possible measurable points are reduced in half. The second method is to collect data by intervening between scattering and background, which would at least be 1 ms apart due to the P43 phosphor screen decay time. In this case, caused by fluctuations, the plasma background signal may not be consistent.

Table 3 Summary of results by considering two different collection lens.

	Magnification Ratio 1:2	Magnification Ratio 1:3
Max. number of fibers (position)	7	11
Collected N_{ph} (N_{pe})	16387 (4407)	7269 (1955)
Spectrometer resolution	28.8 nm	19.2 nm

5. Summary and Conclusions

A summary is given in Table 3 that compare two different settings by the magnification ratio of the collection lens. When observing the lower limit of the TS system based on VPH grating and an intensified camera, both design show significant number of scattered photons. With lower magnification ratio, more points can be measured but with less collection of scattered photons. The resolution bandwidth is rather large compared to typical spectrometers. Although deconvolution is a straight forward method to remove the effect of instrumental broadening, still it is advisable to keep the resolution small.

Being compact and all-in-one unit (intensified camera) does indeed have an attraction in terms of reducing the system complexity and post processing of data. To be conservative, perhaps increasing the laser energy to 2 J/pulse would be beneficial for the scattering signal to overcome background subtraction.

Systems with longer focal length have also been examined. If the magnification ratio of the collection lens is kept identical and matched with the throughput of the optical fiber the same result should appear. In this case, the clear aperture diameter of the collection lens increases.

[1] K.Y. Lee *et al.*, Rev. Sci. Instrum. **89**, 013508 (2018).
[2] T. Yamauchi *et al.*, Phys. Lett. A, **223(3)**, 179 (1996).
[3] C.J. Barth *et al.*, Rev. Sci. Instrum. **68(9)**, 3380 (1997).
[4] D.J. Schlossberg *et al.*, Rev. Sci. Instrum. **87**, 11E403 (2016).
[5] A.C. Selden, Phys. Lett. **79A**, number 5-6, 405 (1980).